Use of In Vitro Data for Construction of a Physiologically Based Pharmacokinetic Model for Naphthalene in Rats and Mice To Probe Species Differences

D. J. Quick[†] and M. L. Shuler*

School of Chemical Engineering, Cornell University, Ithaca, New York 14853

A physiologically based pharmacokinetic (PBPK) model with five tissue groups (lung, liver, fat, richly perfused, and poorly perfused tissues plus venous and arterial blood compartments) has been developed from in vitro data and models of primary cell cultures for naphthalene toxicity in mice and rats. It extends a previous naphthalene PBPK model (Sweeney et al., 1996) and demonstrates a possible approach to a predictive mathematical model that requires minimal animal data. Naphthalene metabolism was examined after four exposure routes (intraperitoneal injection (ip), intravenous injection (iv), ingestion (po), and inhalation). Naphthalene and its primary metabolite, naphthalene oxide, are consumed by enzymes in pulmonary and hepatic tissues (cytochrome P450 monooxygenases, epoxide hydrolase, and glutathione-S-transferase). Additionally, the nonenzymatic reactions of naphthalene oxide in all tissues and in blood are included in the model. Kinetic constants for the model were derived primarily from cell fraction and primary cell culture incubations presented in the literature. The mouse model accurately predicts glutathione (GSH) and covalent naphthalene oxide−protein binding levels after a range of ip doses, and the rat model provides excellent estimates for mercapturate excretion following po doses; but neither model simulates well naphthalene blood concentrations after low iv doses. Good prediction of in vivo response using only in vitro data for parameter estimation (except for epoxide−protein binding rates) suggests that the assumed molecular description is a plausible representation of the underlying mechanisms of toxicity. Mice and rats show significant species differences in response to naphthalene. The model results suggest that species differences in toxicity may be explained, in part, by the lower overall rate of enzyme activities in the rat cells. Lower enzyme activities in the rat result in out-of-phase GSH minima in hepatic and lung compartments, while the simultaneous occurrence of these minima in mice results in higher naphthalene oxide concentrations, thereby allowing formation of more metabolites (e.g., covalent binding to proteins) that may be toxic.

Introduction

As our knowledge of molecular level toxicology increases, it is important to have a method to both test the completeness of our understanding of the underlying biochemical mechanisms and relate those mechanisms to predicting whole animal response. One method to accomplish this is to construct physiologically based pharmacokinetic models (PBPK) using only data from the molecular level experiments. Such an approach may reduce dependence on tests in whole animals.

While PBPK models have been very useful in toxicology (e.g., Andersen et al., 1987), most PBPK models rely heavily on fitting parameters to in vivo data and this requires extensive animal studies. Fitting to in vivo data is a less stringent test of the validity of a proposed mechanism than determining all parameters for a proposed mechanism independently using in vitro data and then predicting in vivo response. While toxicological studies on humans are problematic, studies on isolated human cells or cell fractions are easily accessible. Approaches that rely on in vitro data but can make useful predictions on an in vivo basis would be important in cross-species extrapolation and to prediction of exposure risks for humans.

PBPK models are particularly enlightening when the drug/toxin is known to have organ-specific activity or has shown species specificity. A toxin which has exhibited both of these characteristics, naphthalene, was chosen for the current analysis. Naphthalene metabolism is also representative of a broad class of non-nutritive hydrocarbons.

Naphthalene is a prevalent environmental contaminant resulting from cigarette smoke, moth balls, combustion of fossil fuels, and the production of dyes and is known to cause cataracts and hemolytic anemia in humans (Toxicological Profile, 1990). Interestingly, low doses of naphthalene are fatal to mice (380 mg/kg ip LD_{50}: Shank et al., 1980; 350 mg/kg oral LD_{50}: Plasterer et al., 1985) whereas much larger doses can be tolerated by rats (1600 mg/kg ip LD_{50}: Plopper et al., 1992; 2300

[†] Present address: SmithKline Beecham, 709 Swedeland Rd., P.O. Box 1539, King of Prussia, PA 19406.

* Corresponding author. Address: 270 Olin Hall, School of Chemical Engineering, Cornell University, Ithaca, NY 14853. Telephone: (607) 255-7577. Fax: (607) 255-1136.

10.1021/bp990057t CCC: $18.00
Published on Web 05/04/1999

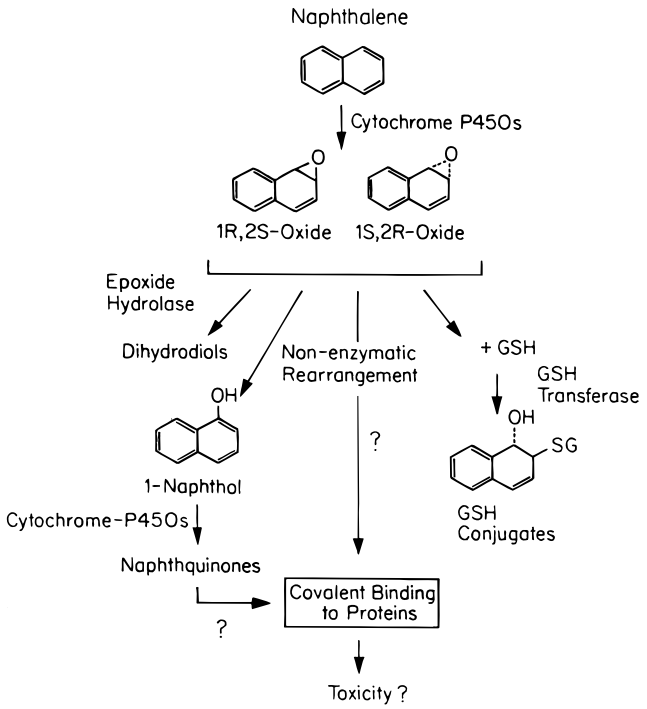

Figure 1. Reaction scheme for naphthalene and its products.

mg/kg oral LD_{50}: Gaines et al., 1969). In mice pulmonary cytotoxicity appears to be the cause of death (Buckpitt et al., 1995), unlike rats where death follows liver failure (Germansky and Jamall, 1988). The cause of this species difference has not been determined.

Metabolism of naphthalene occurs via the same pathways as many other aromatic hydrocarbons (general review: Buckpitt and Franklin, 1989), and a PBPK model for naphthalene should be representative of a class of models for other non-nutrient hydrocarbons.

Naphthalene is metabolized by the cytochrome P450 monooxygenase system into reactive metabolites. The primary site of naphthalene metabolism is the liver, where it is metabolized into naphthalene oxide enantiomers. The lung contains lower levels of monooxygenase activity overall compared to the liver, but that activity is highly localized in the Clara cell, which may be one of the reasons why they are so susceptible to naphthalene-induced damage. Naphthalene oxide can then undergo further metabolism: conjugation to glutathione (GSH) by glutathione transferase, conversion to dihydrodiol by epoxide hydrolase enzymes, spontaneous rearrangement to form 1-naphthol or covalent binding to macromolecules. Further, 1-naphthol can be converted by some P450 isoforms into 1,2-naphthoquinone and 1,4-naphthoquinone, which can react with proteins. Toxicity is likely associated with epoxide or quinone binding to protein. Naphthalene metabolism in rodents is summarized in Figure 1 (based on Kanekal et al., 1991).

Naphthalene forms two reactive metabolite enantiomers: (1*R*,2*S*)-naphthalene oxide and (1*S*,2*R*)-naphthalene oxide. Three glutathione conjugates (of a possible four) have been identified by HPLC and have been labeled according to their peaks as conjugates 1, 2, and 3 (Buonarati et al., 1990). The (1*S*,2*R*)-naphthalene oxide enantiomer forms conjugates 1 and 3, while (1*R*,2*S*)-naphthalene oxide forms conjugate 2. Incubations of naphthalene with mouse lung and liver microsomes indicate that mouse lung microsomes preferentially form the (1*R*,2*S*)-naphthalene oxide enantiomer (Buckpitt et al., 1987). The rate of metabolism to epoxide was much lower in rat and hamster lung microsomes than in the mouse, and stereospecificity of epoxidation was not observed. More recently Fanucchi et al. (1997) have shown that steroselective activity corresponds to CYP2F2 protein expression. Stereospecificity of epoxidation does not occur in nontarget tissues or species and may play a role in the selective cytotoxicity of naphthalene. It is believed that circulating reactive metabolites formed in one organ (i.e., the liver) *may* be responsible for cell death in another organ (i.e., the lung), at least in the mouse. Kanekal et al. (1990, 1991) have summarized much of the evidence supporting the hypothesis that a reactive metabolite generated in the liver results in lung damage. An alternative explanation is that the reactive metabolites generated in the Clara cells lead to cell death and differences between the mouse and rat reflect intrinsic differences in activation and or sensitivity.

Recent experiments by Zheng et al. (1997) show that 1,2-naphthoquinone is a reactive metabolite that will bind with specific proteins from the mouse Clara cell. Also Wilson et al. (1996) found that 1-naphthol incurs metabolism-dependent cytotoxicity in a system with human liver microsomes and human MNL (mononuclear leucocytes) with the cytotoxic products being 1,2- and 1,4-naphthoquinones. Although this recent in vitro data links the further metabolism of 1-naphthol to toxicity, earlier studies found no lung injury after administration of 1-naphthol in vivo (Buckpitt et al., 1985).

Thus, the role in toxicity of naphthol and its subsequent bioactivation to quinones is unclear. The decomposition of epoxide to naphthol in in vitro systems in cell culture medium is much more rapid than in medium with serum albumin (Kanekal et al., 1991) and presumably much more rapid than in blood. This difference in epoxide stability may make toxicity due to quinones much more apparent in vitro than in vivo. Since in vivo experiments with rodents directly dosed with 1-naphthol show no toxicity (Buckpitt et al., 1985), we ignored in the PBPK model the conversion of 1-naphthol to quinones. However, discrepancies among in vitro data sets could be the result of differences in conversion of epoxides to 1-naphthol due to differences in composition of culture medium or in the time elapsed between sampling and analysis.

Sweeney (1993) and Sweeney et al. (1996) examined the effects of naphthalene exposure on mice and rats with a PBPK model. Biochemical parameters for this preliminary PBPK model, incorporating pulmonary and hepatic metabolism of naphthalene and naphthalene oxide, were estimated entirely from the literature. Although these kinetic parameters sufficiently predicted earlier data from cell fraction and animal experiments, the more recently published, more complete data set (Buckpitt et al., 1992) cannot be matched with these kinetic parameters, and revision of the preliminary model is necessary.

In this paper, a naphthalene/naphthalene oxide PBPK model is presented which includes five lumped tissue compartments (lung, liver, fat, richly perfused, and poorly perfused) and two blood compartments (venous and arterial) that are assumed to be well-mixed and flow-limited (i.e., organs in equilibrium with blood exiting the organ). Models written for a mouse and a rat allow naphthalene exposure via inhalation, intravenous (iv) injection, intraperitoneal (ip) injection, and ingestion (po). The primary objective is to describe a modeling approach that may be generally effective for predicting in vivo response to nonnutrient hydrocarbons using almost exclusively in vitro data from cell fractions and primary cell cultures. Model predictions are compared to literature data including naphthalene blood concentrations

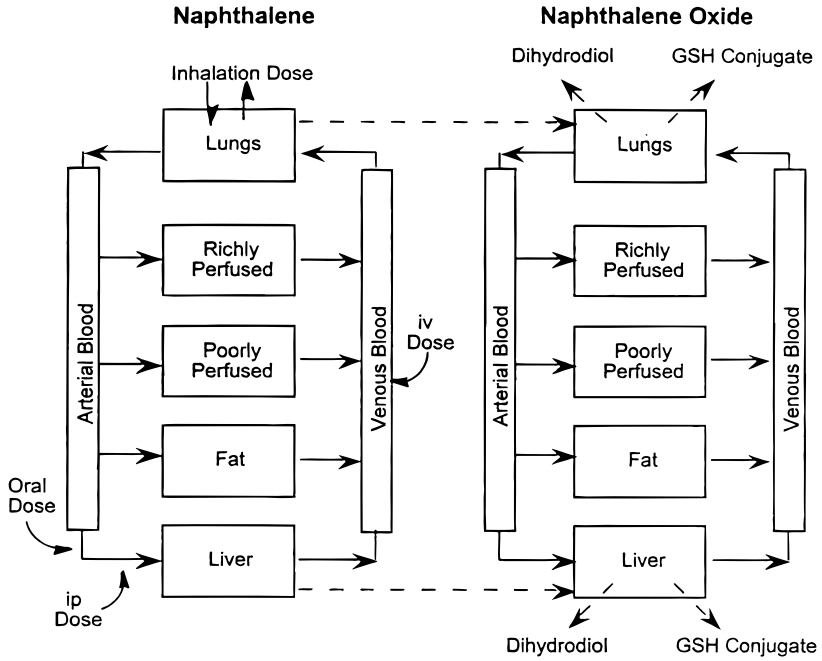

Figure 2. Schematic of the tissue and blood compartments included in the PBPK model.

after low iv doses, GSH and naphthalene oxide binding levels produced by a large range of ip doses, GSH levels and mercapturate excretion following oral doses, and pretreatment with a GSH depleting agent. These predictions are then used to probe a possible mechanism for the species difference between mice and rats in response to naphthalene exposure.

Development of the PBPK Model

Model Structure. A flow diagram of the five well-mixed, venous equilibrated tissue compartments in the PBPK model is shown schematically in Figure 2. The equations comprising the model are presented in the Appendix. The conversion of naphthol to quinones is ignored in the model, as this reaction is reported to be negligible in vivo (Buckpitt et al., 1985) and the amount of naphthol generated in the model is small so the level of any reaction products would be small. The assumption that each organ acts as a well-mixed compartment was tested by comparing model results assuming a single compartment for each organ to models where the organs were modeled as a variable number of well-mixed compartments in series. For naphthalene, models with a single compartment or multiple subcompartments gave nearly identical predictions (Quick, 1996) and the organs were subsequently modeled as single well-mixed compartments.

Determining Kinetic Parameters from Cell Fraction Data. The majority of the experimental analysis of naphthalene metabolism has been performed with microsomal and cytosolic fractions of mouse and rat cells (data in Buckpitt et al., 1984, 1987, 1992). Such data provide a first estimate for the rate constants controlling the biochemical reactions responsible for metabolizing naphthalene in an animal. To determine values from the several experiments conducted with varying amounts of microsomal and cytosolic cell fractions and conducted at different naphthalene concentrations, a parameter-fitting routine was written (Quick, 1996).

The fitting routine for cell fractions, a set of differential equations describing metabolism of naphthalene and naphthalene oxide by microsomes, cytosolic proteins, and nonenzymatic reactions, minimizes the percent error in predicted metabolite concentrations (defined as (predicted − measured)/measured × 100) by making fractional changes in rate parameter values. The differential equations describing metabolism in this and all subsequent programs were solved simultaneously by numerical integration using the program LSODA (Livermore Solver of Ordinary Differential Equations, with Automatic switching method for stiff and nonstiff problems, L. R. Petzold and A. C. Hindmarch, Lawrence Livermore Laboratory, Livermore, CA). All of the FORTRAN computer programs were run on a Unix workstation.

Many of the reported experiments were conducted with purified glutathione-S-transferase (GST) rather than with cytosolic cell fraction; thus for analysis with the parameter-fitting routine GST activity was related to cytosolic protein. Incubations of 1 mg/mL mouse liver microsomal protein with varying levels of GST purified from mouse liver cytosol (Buckpitt et al., 1992) and also with varying levels of mouse liver cytosolic protein (Buckpitt et al., 1984) suggest that 5 CDNB (1-chloro-2,4-dinitrobenzene) units of liver GST is equivalent to about 2 mg of liver cytosolic protein. The relationship between the two types of experiments is less certain for similar experiments with mouse lung components, however 5 CDNB units of GST purified from lung cytosol is approximately equivalent to 2 mg of lung cytosolic protein. The same equivalencies were assumed for rat lung as for mouse lung cytosolic fractions and for rat liver as for mouse liver cytosolic fractions.

For estimating rate constants for the mouse lung and mouse liver, parameters were fitted to data from microsomal incubations with purified GST and varying amounts of naphthalene and GSH (Buckpitt et al., 1992) using the parameter-fitting routine. For the rat lung, parameters were fitted to the same data set. For the mouse lung, mouse liver, and rat lung, the error between the fit and the data was 16%, 15%, and 7%, respectively. For the rat liver, parameters could not be fit using the fitting routine due to insufficient data.

Reconciling Values of Cell Fraction Kinetic Parameters with Whole Cell Data. A key difference

Table 1. Cell Characteristics[a]

	Clara cell	hepatocyte
C_x^{GSHss} (μM)	310[a]	7500[b]
k_x^{GD} (1/min)	0.00055[c]	0.0055[c]
cells (no./mL of organ)	2.7×10^{8} [d]	1.1×10^{6} [e]
cell volumes (μm^3)	366[d]	4940 [f]
organ volume (%)	9.6[d]	not used
total protein (mg/mL of organ)	92 (lung)[g]	192 (liver)[g]

[a] Calculated as described in the text. [b] Cho et al. (1994a). [c] Griffith and Meister (1979). [d] Haies et al. (1981). [e] Seglen (1973). [f] Weibel et al. (1969). [g] Knox (1972).

between the present model and the preliminary version of this work is the use of data accumulated from primary cells (Clara cells from the lung and hepatocytes from the liver) cultured in the presence of naphthalene and its oxides. To use cell culture results, a model of stationary cultured cells was written incorporating key biochemical reactions and assuming the exchange of intracellular and extracellular concentrations of naphthalene to be rapid, and thus in equilibrium (Quick, 1996).

The cell model consists of a set of differential equations describing metabolism of naphthalene and naphthalene oxide by microsomes, cytosolic proteins, and nonenzymatic reactions in a plated cell culture. Since some of the metabolic reactions can only occur inside the cell (where the enzymatic proteins are located), the model treats the cells and medium as two distinct elements of the cell culture. The cells are modeled as a single unit containing the sum of the components of all the individual cells. Two reactions are assumed to occur in the medium (binding of naphthalene oxide to medium proteins and formation of 1-naphthol from naphthalene oxide), and five reactions are assumed to occur in the cells (formation of naphthalene oxide from naphthalene and subsequent reactions of naphthalene oxide: binding to cell proteins, formation of 1-naphthol, conversion to dihydrodiols, and conjugation to cellular glutathione).

Since the cells and medium are considered as separate compartments in the model, the transfer of naphthalene and its oxides between the two compartments must be included in the model. The ratios of naphthalene and naphthalene oxide concentrations intracellularly versus extracellularly are assumed to be governed by equilibrium partition coefficients. The same partition coefficients are assumed for incubated murine Clara cells or hepatocytes as those determined for the mouse PBPK model for the exchange between blood and lung or liver tissue, respectively.

When the equations were written for each individual compartment, we had difficulty obtaining stable solutions. Equations 18, 19, 21, and 22 are written on an overall system basis. By taking advantage of the equilibrium between compartments (e.g., partition coefficients) equations could be derived for each species in the separate compartments. This approach accounts for the $1/[VC_x + VM_x/P_x]$ term in eqs 18 and 19 and for the $[P_xVC_x + VM_x]$ term in eqs 21 and 22. This approach resulted in a model amenable to solution.

General cell characteristics necessary for the use of cell models (including cell size, number of cells per organ, protein per cell, and GSH level) have been reported (Table 1). The total protein per cell was calculated from reported values of milligrams of protein per milliliters of organ and the number of cells per milliliters of organ. Calculating protein per Clara cell required an additional piece of information: the percentage of the organ volume which is made up by Clara cells. While GSH concentration in the hepatocytes was assumed to be the same as that reported for liver tissue, GSH has been reported for Clara cells on a per cell basis (Chichester et al., 1994) and was multiplied by the reported volume of the Clara cell to obtain the GSH concentration for the cell culture model.

Rate constants determined for cell fractions on a per milligram of microsomal protein basis (V_{max} values for P450 and EH), on a per milligram of cytosolic protein basis (V_{max} for GST), or on a per milligram of total protein basis (first-order rate for covalent binding) must be multiplied by the appropriate protein content of the cell to use them in the cell culture models. For example, the initial $V_{max_{P450}}$ in the hepatocyte model was determined by multiplying the $V_{max_{P450}}$ fit to the mouse liver cell fractions by the milligram of microsomal protein per milliliter of hepatocytes.

An exception to this rule is the factor multiplied by $V_{max_{GST}}$. The rate of conjugation of naphthalene oxide to glutathione reaches a constant value with the addition of cytosolic protein greater than half the amount of microsomal protein when using mouse lung cell fractions (Buckpitt et al., 1984). For mouse liver cell fractions, conjugation seems to saturate at around a one-to-one ratio of proteins. While the actual ratio of cytosolic to microsomal protein reported for rat liver is about 3 to 1, the $V_{max_{GST}}$ values used in both the cell and PBPK models were based on the aforementioned fractions of "effective" cytosolic protein rather than the estimated total amount of cytosolic protein. The saturation of the response by cytosolic protein, which is proportional to GST levels, suggests a limitation in the rate of generation of one of the substrates or the addition of competing substrates and reactions with additional cytosol. It is likely that this in vitro reconstruction is not fully representative of in vivo.

An additional requirement for the cell models was a description of normal glutathione turnover. Parameters for GSH resynthesis and the mechanism of resynthesis were estimated independently of the cell model. GSH was assumed to be resynthesized at a rate equal to the product of the steady-state level of GSH and the first-order degradation rate of GSH. Degradation rates of GSH have been reported for mouse lung and liver tissues (Griffith and Meister, 1979) and rat lung and liver tissues (Frederick et al., 1992). These rates (in units of μM/h/(μM steady-state GSH)) were assumed to be the same in isolated cells as reported for animal tissues.

There were no data available for comparison to a rat lung or liver cell model; thus, only mouse cell models were written. The mouse lung cell model incorporating parameters fit to the lung cell fractions was insufficient at fitting data from Clara cells dosed with naphthalene oxide (Chichester et al., 1994) due to the apparent stereospecificity of GSH conjugate production (not observed with lung cell fractions and thus not included in the cell model equations). Clara cells incubated with naphthalene (Chichester et al., 1994) show a higher *RS*/*SR* conjugate ratio (partially due to GST stereoselectivity, but probably also resulting from enhanced P450 stereoselectivity) and form much more product (about 100× more) than lung cell fractions (primarily in the form of covalent binding to proteins). Thus P450 V_{max} and K_m values previously fit to lung cell fractions were modified to match the *RS*/*SR* conjugate ratio of the Clara cell, and the P450 V_{max} values were increased to match the quantity of products formed in the Clara cells.

For the mouse liver cell model, the rate constants fit to the mouse liver cell fractions gave fair predictions of the dihydrodiol and GSH conjugate formation in hepa-

Table 2. 22 g Mouse Kinetic Parameter Values[a]

kinetic parameter	lung RS	lung SR	liver RS	liver SR
$V_{max_{P450}}$ (μM/min)	8.75	17.5	118	210
$K_{m^{N}_{P450}}$ (μM)	2.1	800	7.0	115
$V_{max_{EH}}$ (μM/min)	26.5	20.5	336	134
$K_{m^{NO}_{EH}}$ (μM)	4.0	0.4	21	9.0

parameter	lung	liver
$V_{max_{GST}}$ (μM/min)	2750	2800
K3 (μM)	35	35
K2 (μM)	3800	2100
K1 (μM^2)	310000	150000
k_x^{GD} (1/min)	0.00055[b]	0.0055[b]
C_x^{GSHss} (μM)	1800	7500

naphthol formation in all tissues and blood

k_{NOH} (μM/μM NO/min) 0.173 exp(−20.2 × total protein)

protein and binding rate	lung	liver	fat	richly	poorly	blood
total prot. (mg/mL of tissue)	92	192	44	180	200	55[c]
microsomal (mg/mL of tissue)	5.0	28	---	---	---	---
active cytosolic (mg/mL)	2.5	28	---	---	---	---
k_b (μM /min)	0.11	0.077	0.018	0.22	0.08	1.05

[a] Determined as described in text unless otherwise noted. [b] Griffith and Meister (1979). [c] Crispens (1975).

Table 3. 220 g Rat Kinetic Parameter Values[a]

kinetic parameter	lung RS	lung SR	liver RS	liver SR
$V_{max_{P450}}$ (nmol/mg of mp/min)	0.93	0.85	0.34	1.4
$K_{m^{N}_{P450}}$ (mM)	38	9.0	7.0	115
$V_{max_{EH}}$ (nmol/mg of mp/min)	9.8	6.5	10.3	4.1
$K_{m^{NO}_{EH}}$ (mM)	9.0	25	21	9.0

parameter	lung	liver
$V_{max_{GST}}$ (nmol/mg of cp/min)	650	43
K3 (μM)	35	35
K2 (μM)	3800	2100
K1 (μM^2)	150000	150000
k_x^{GD} (1/min)	0.00018[b]	0.0024[b]
C_x^{GSHss} (μM)	2000	6000

naphthol formation in all tissues and blood

k_{NOH} (μM/μM NO/min) 0.173 exp(−20.2 × tp)

protein and binding rate	lung	liver	fat	richly	poorly	blood
total prot. (mg/mL of tissue)	92	192	44	180	200	55[c]
microsomal (mg/mL of tissue)	5.0	28	---	---	---	---
active cytosolic (mg/mL)	2.5	28	---	---	---	---
k_b (pmol/mg of tp/min)	1.2	0.4	0.4	1.2	0.4	19.0

[a] Determined as described in text unless otherwise noted. Note: mp = microsomal protein, cp = cytosolic protein, tp = total protein. [b] Frederick et al. (1992). [c] Knox (1972).

tocytes incubated with naphthalene oxide (Buonarati et al., 1989). Hepatocytes incubated with naphthalene (Richieri and Buckpitt, 1987) show a smaller *RS*/*SR* conjugate ratio than liver cell fractions and a considerably different ratio of dihydrodiol to GSH conjugate products. As with Clara cells, the P450 V_{max} and K_m values fit to the cell fractions were modified to match the *RS*/*SR* conjugate ratio of the cell; for hepatocytes, however, the magnitudes of products formed in cell fractions and by the hepatocytes were similar.

Kinetic Parameters: PBPK Values. The final step in establishing kinetic parameters for the PBPK models involved combining information gained from fitting parameters to cell fraction data with that obtained from the cell models.

Although cells may better represent in vivo metabolism than cell fractions, not all of the parameters fitted with the cell models were used in the mouse PBPK model. Since Clara cells make up less than 5% of the lung cell population, some of the parameters fitted to the Clara cell model would be inappropriate for modeling the mouse lung tissue compartment. For example, the increased P450 V_{max} values necessary to match the magnitude of products formed by the Clara cells would be too high to represent the V_{max} of the whole mouse lung. However since the Clara cells are a primary site of naphthalene metabolism in the lung, the relative P450 V_{max} values determined to match the *RS*/*SR* ratio of the Clara cell were assumed to be representative of lung metabolism. Also the rate of epoxide binding determined with the Clara cell was assumed not to be indicative of the binding that would occur in the remaining lung cells. Thus for the lung compartment of the mouse PBPK model, 12 rate constants were determined with the parameter fitting routine and the cell model, one rate constant was estimated independently of cellular or cell fraction data (naphthol formation), and the rate of epoxide binding to proteins was set to match reported in vivo binding levels (Table 2).

For the mouse liver compartment of the PBPK model, 12 rate constants were determined with the parameter fitting routine and the cell model and one rate constant was estimated independently of the cellular or cell fraction data (naphthol formation). The rate of covalent binding in the liver compartment was estimated from reported binding levels in incubations of hepatocytes with naphthalene oxide (independent of the cell model) (Table 2).

In the absence of rat lung cell data, the parameters fit to the microsomal cell fractions were used in the lung compartment of the rat PBPK model (Table 3).

For the rat liver, parameters could not be fit using the fitting routine for cell fraction data or a cell model due to an insufficient quantity of data over a range of naphthalene concentrations. Rat liver rate constants were thus determined from data presented in Buckpitt et al. (1987) and O'Brien et al. (1985) in conjunction with the results of mouse liver parameter fitting. These two papers compare metabolism by mouse and rat microsomes. Starting with the parameters fitted to the mouse liver cell fractions, the V_{max} values were reduced according to ratios of products formed from mouse and rat liver cell fractions (K_m values were assumed unchanged). P450 parameters were determined using the ratios of rat to mouse total products formed (47%: Buckpitt et al., 1987; 22%: O'Brien et al., 1985); the percentage giving the best comparison to the animal data was used in the model (22%). In addition to differences in total product formation, the ratio of enantiomer production differs greatly between rat and mouse liver cell fractions. Thus the $V_{max_{P450}}$ for the *RS* oxide was increased and the $V_{max_{P450}}$ for the *SR* oxide was decreased to match the observed rat liver cell fraction *RS*/*SR* ratio while maintaining the appropriate total product formation. The V_{max} values for conjugate and dihydrodiol formation in the rat liver were taken as 43% and 86% of the values for the mouse liver, respectively, as suggested by the data in Buckpitt et al. (1987).

Table 4. Parameters Used in Naphthalene PBPK Model

22 g Mouse[a]
total blood volume: 1.87 mL[b]; venous blood: arterial blood ratio 2:1[c]

	organ volumes (mL)	blood flow (mL/min)	tissue: blood PC (−)
lung	0.33[d]	15.1[e]	1.55[f]
liver	0.88	3.78	4.96[f]
fat	0.88[c]	0.75	103[f]
well perfused	1.1	7.7	2.82[f]
poorly perfused	17.2	2.87	3.82[f]

220 g Rat[c]
total blood volume: 13.2 mL; venous blood: arterial blood ratio 2:1

	organ volume (mL)	blood flow (mL/min)	tissue: blood PC (−)
lung	2.53	76.2	1.55[f]
liver	8.80	19.0	4.96[f]
fat	15.4	6.9	103[f]
well perfused	8.5	38.9	2.82[f]
poorly perfused	165	11.4	3.82[f]

[a] Andersen et al. (1987), unless otherwise noted. [b] Wish et al. (1950). [c] Gearhart et al. (1990). [d] Crosfill and Widdicombe (1961). [e] Ramsey and Andersen (1984). [f] Determined as described in text.

The mouse liver parameters which were fitted to data in Buckpitt et al. (1992) predict about half of the total metabolite formation observed in Buckpitt et al. (1987) and about twice that observed in O'Brien et al. (1985). No single set of parameters can fit all three data sets, showing inconsistency among these data sets. Thus to determine appropriate rat $V_{max_{P450}}$ parameters, values were selected to predict twice the metabolism reported in O'Brien et al. (1985) and half the metabolism in Buckpitt et al. (1987). The V_{max} values related to the data in O'Brien et al. (1985) compared more favorably with the available in vivo rat data. The parameters fitting the rat liver cell fractions are used in the rat PBPK model and are provided in Table 3.

Physiological Parameters. The compartment volumes and flow rates are based on reported organ sizes, blood volume, and blood flow rates to each of the organs. The values used in this model are taken as the experimentally observed value closest to an average of the reported values found in the literature (Table 4).

Protein concentrations in the tissues have been reported for the rat (lung, liver, kidney, and muscle tissues) and human (adipose tissue: Duck, 1990) (Table 3). Total protein for the richly perfused compartment is assumed to be the same as that reported for the kidney, and values for the muscle tissue are assumed to be representative of the poorly perfused tissues. Microsomal protein in the rat lung is an average of three reported values (Johanneson et al., 1977; Rietjens et al., 1988; Seidegard et al., 1977). The same protein concentrations were used for the mouse (Table 2) as have been reported for the rat and human. The average amount of protein reported for mouse blood was also used in the rat model.

Partition Coefficients. Inherent to the assumption of a flow-limited PBPK model is the assumption that naphthalene will partition from the tissues according to thermodynamic equilibrium into the exiting blood stream. The partition coefficients (PCs) for naphthalene exchange are estimated from the octanol:water (Hansch and Leo, 1979) and water:air PCs (CRC Handbook, 1990) for naphthalene using the regression equations in Abraham et al. (1985) and Fiserova-Bergerova and Diaz (1986) (see Table 4).

Animal experiments (Tsuruda et al., 1990) confirm that naphthalene oxide circulates (as suggested by previous studies with isolated hepatocytes: Richieri and Buckpitt, 1987); thus, naphthalene oxide must partition from the organs into the blood. Since octanol:water and water:air PCs have not been reported for naphthalene oxide, the PCs for naphthalene oxide cannot be estimated as they were for naphthalene. Instead the PCs are assumed to be the same as those determined for naphthalene in all tissues except the fat. This assumption is based on analogy to other systems with circulating epoxides. The PCs used in PBPK models for styrene/ styrene oxide (Csanády et al., 1994), and butadiene and its monoepoxide (Medinsky et al., 1994) contain similar measured tissue: blood PCs for the parent compound and the oxide metabolite in all tissues but the fat. For the fat tissue the parent compound has a much larger PC (5−7 times greater). Thus the fat:blood PC for naphthalene oxide was assumed to be 6 times less than that determined for naphthalene (Table 4).

Exposure Routes. The PBPK model incorporates naphthalene exposure by one of several routes (see Appendix). For ip injection, all of the naphthalene dose is assumed to be absorbed by the liver in 1 min (eq 3). For iv dosing, the naphthalene dose is assumed to be distributed throughout the venous blood compartment in about 2 s (eqs 16 and 17). For po dosing, the naphthalene dose is assumed to be absorbed with a half-life of 0.5 h (eq 3). This half-life has previously been used in a PBPK model for styrene (Csanády et al., 1994). Also, as for styrene, all of the naphthalene dose is assumed to enter the circulation from the gastrointestinal tract (100% bioavailability).

Results

Mouse PBPK Model. The mouse model makes reasonably accurate predictions of in vivo GSH and binding levels 4 h after naphthalene ip doses ranging from 10 to 600 mg/kg (Figure 3). The only predictions falling outside of the literature values are at high doses where the predicted binding of naphthalene oxide to proteins in the lung is less than observed and in the liver it is slightly greater than observed.

The model predictions compare reasonably well to observed GSH depletion over time (Figure 4); however, the model is unable to accurately predict the observed lung GSH resynthesis after 240 min. GSH levels in the liver are predicted fairly well; however, more liver GSH depletion is predicted in response to the 200 mg/kg dose than is observed. Decreasing liver $V_{max_{P450}}$ to 40% of its initial value provides excellent agreement through 240 min. The match to liver GSH resynthesis does not necessarily suggest that the GSH resynthesis model is accurate. When the P450 parameters are modified ($0.4V_{max_{P450}}$) to match liver GSH depletion (Figure 4), GSH resynthesis is underpredicted at long times (480 min). An alternate GSH resynthesis description (as proposed in D'Souza et al., 1988) would probably better describe GSH resynthesis, but new experiments would be needed to independently determine kinetic parameters for the proposed mechanism.

Despite good comparison to GSH and binding levels at many doses, the model predictions compare only fairly well to naphthalene in the blood over time after iv doses (data taken from NTP Task No. Chem00646 (1995)) (see Figure 5). Good comparison to most of the available data with only fair comparison to naphthalene concentrations in the blood suggests that the descriptions of mass

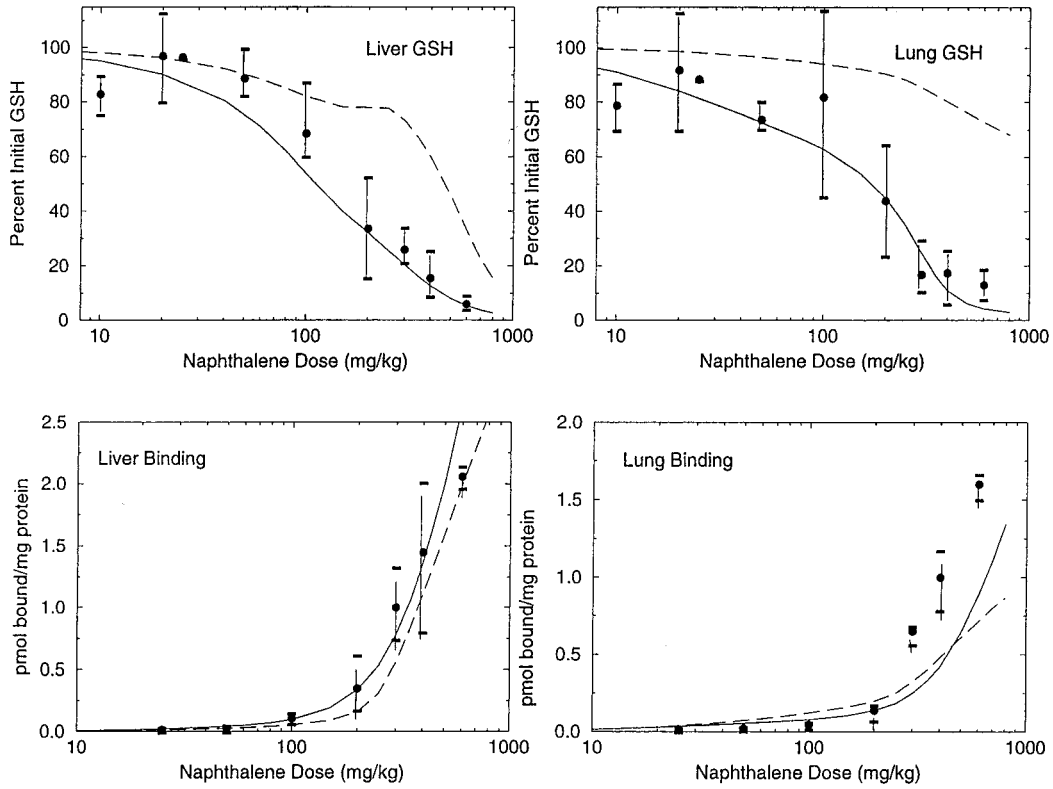

Figure 3. Effects of ip dosing of naphthalene on GSH depletion and on the level of epoxide binding in the mouse lung and liver 4 h after dosing. The average value of reported data and range of response (Φ) is compared with predictions from the model of Sweeney et al. (1996) (- - -) and the model presented in this paper (—).

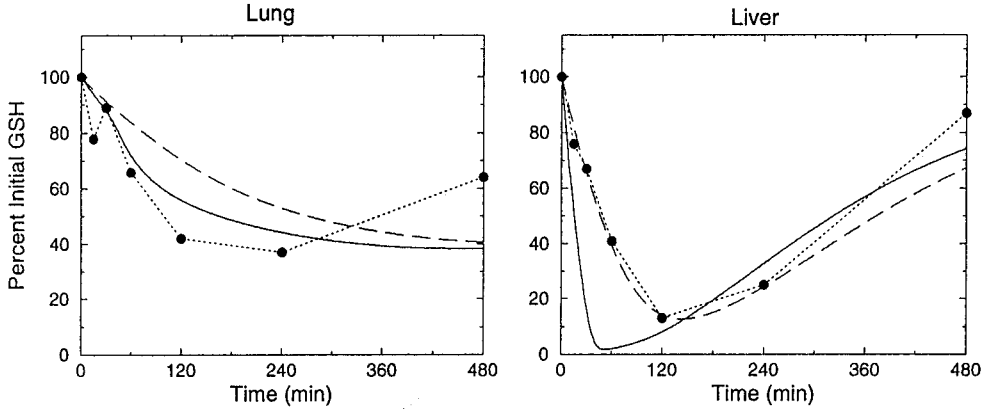

Figure 4. Prediction of time-dependent GSH depletion in mouse lung and liver in response to an ip dose of 200 mg/kg. Data from Warren et al. (1982) (•••) are compared to prediction of the model (—) and the model modified with a liver $V_{max_{P450}}$ value multiplied by 0.4 (- - -).

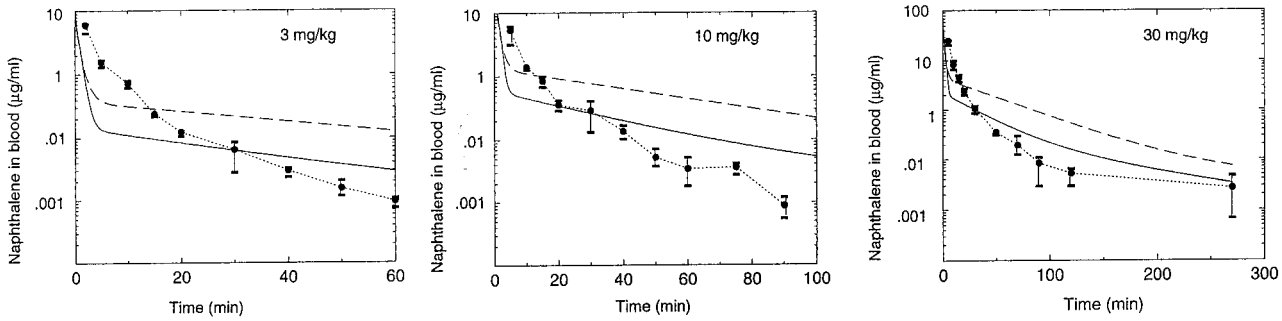

Figure 5. Prediction of time-dependent naphthalene levels in the blood of the mouse for three different iv naphthalene doses (3, 10, and 30 mg/kg of body weight). Data (●) from a NIEHS study (NTP Task No. Chem 00646, 1995) are compared to the model (—) and the Sweeney et al. (1996) model modified for iv dosing (- - -).

Table 5. Effects of BSO Pretreatment

	GSH (% control)		bound (nmol/mg of tp)	
	lung	liver	lung	liver
no BSO[a]	39.5	16.3	0.14	0.25
with BSO[a]	15.5	3.9	0.42	1.06
predicted (no BSO)	44.8	32.3	0.138	0.338
predicted (with BSO)	18.1	7.21	0.281	0.867

[a] Buckpitt and Warren (1983).

transfer and/or dose uptake in the model may be inadequate. Experiments show naphthalene slowly and steadily being absorbed from the blood and subsequently metabolized in the tissues, while model predictions show a surge in naphthalene uptake and metabolism by the tissues.

Although the model does not include explicitly further reaction of the GSH conjugates, estimates could be made for the amount of GSH conjugate metabolites excreted. GSH conjugates are the precursors for mercapturates (mercapturic acids), a primary naphthalene excretion product (Stillwell et al., 1982; Chen and Dorough, 1979). Experiments have demonstrated that 8 h after dosing with each of the three commonly formed GSH conjugates, 69−75% of a conjugate 1 (an *SR* conjugate) dose, 76−84% of a conjugate 2 (the *RS* conjugate) dose, and 39−57% of a conjugate 3 (another *SR* conjugate) dose, were excreted as mercapturates from mice dosed with the individual GSH conjugate isomers over a range of doses (Buonarati et al., 1990). Since the model predicts how much *RS* and *SR* conjugates are formed, an estimate for the amount of naphthalene excreted as mercapturates was made by multiplying the amount of *RS* conjugate formed at any time by 76−84% and multiplying the amount of *SR* conjugate formed at any time by 39−75%. The amount of conjugate excreted after 8 h was similar to the amount excreted over 24 h (Buonarati et al., 1990); thus the *RS* and *SR* conjugate composition of the 8 and 24 h urine samples were assumed similar. Only one value has been reported for naphthalene mercapturates excreted by the mouse (Stillwell et al., 1982). Twenty-four hours after dosing with 100 mg/kg ip naphthalene, 39% of the dose was excreted as mercapturates. The model predicts 34.5%−43.7%.

Yet another test of model validity is comparison to data taken from animals pretreated with chemicals having known effects. Buthionine sulfoximine (BSO) is known to deplete GSH by blocking synthesis for about 2 h (Griffith and Meister, 1979). After 2 h, GSH levels hold constant at a reduced level for about 4 h. In Buckpitt and Warren (1983), mice dosed subcutaneously (sc) with 880 mg/kg BSO were found to have GSH levels of 86% and 35% of control lung and liver levels, respectively, 2 h after dosing. Mice dosed ip with naphthalene 2 h after an sc BSO dose show markedly different GSH and binding levels than control mice dosed with naphthalene. To mimic BSO pretreatment with the model, initial GSH levels were set to be 86% (lung) and 35% (liver) of the GSH levels used in the base model and zero-order GSH synthesis was assumed to occur at a rate equal to the product of the GSH degradation rate and the initial GSH level. Model predictions for lung and liver GSH and binding levels 4 h after a 200 mg/kg ip naphthalene dose (given 2 h after an sc 880 mg/kg BSO dose) are compared to the observations in Table 5. The model accurately predicts the effects of BSO pretreatment on GSH levels but does not predict quantitatively the observed 4-fold increase in binding of naphthalene oxide to proteins. Binding is predicted to increase only about 2-fold.

Models were created to predict exposure to naphthalene via injection, ingestion, or inhalation. Whether naphthalene is injected into the vein (iv) or peritoneum (ip), the model predicts very similar effects (Figure 6). For an oral dose of 200 mg/kg, the slower uptake after oral dosing reduces GSH rebound in the liver; however, lung predictions are similar. Exposure to 130 ppm (about 200 mg/kg) naphthalene has a significantly different effect on GSH depletion in the lung and liver.

Rat PBPK Model. Much less data exist for comparing rat model predictions to experiments. Only O'Brien et al. (1985) show the effects of dosing rats with naphthalene intraperitoneally. The rat PBPK model predicts GSH levels 4 h after ip dosing fairly accurately (Figure 7) and much better than in Sweeney et al. (1996). The underprediction of liver GSH may indicate a poor description of ip dose uptake rather than a poor kinetic description as there is good agreement to other data. Predicted lung GSH levels at the three doses tested compare well to measurements.

Model predictions for naphthalene removal from the blood in the rat compare reasonably well to experiments (Figure 8). The comparison is better than predictions made with the mouse model (seen in Figure 5); however, both models predict a more rapid initial uptake of naphthalene than observed. For the rat model, the predicted blood concentrations are accurate after the first 60 min (particularly at the highest dose tested) and most importantly show a similar slope at long times (indicating a similar long-term rate of naphthalene removal from the blood).

Using the oral dosing model for rats, the predictions compare extremely well to the two reported values of GSH depletion (Table 6). The excellent comparison

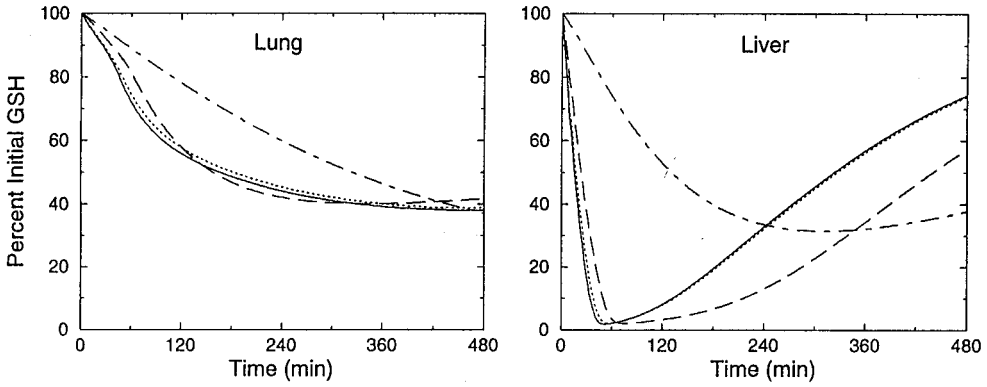

Figure 6. Effects of dose route on GSH depletion in the mouse at a naphthalene dose of 200 mg/kg or equivalent. Comparisons are of ip injection (—), iv injection (···), oral dosing (- - -), and inhalation of 130 ppm naphthalene (-·-).

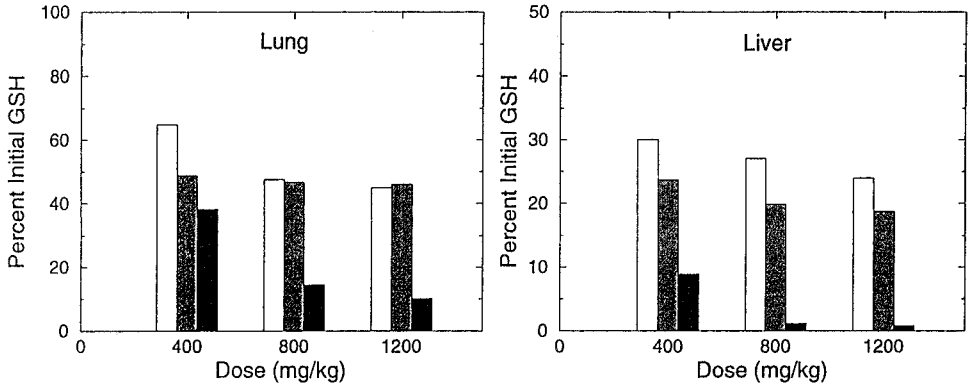

Figure 7. Effects of an ip naphthalene dose on GSH depletion in the rat lung and liver. The empty bars represent values from O'Brien et al. (1985); the shaded bars are the levels predicted with the current model; and the solid bars represent predictions from the model of Sweeney et al. (1996).

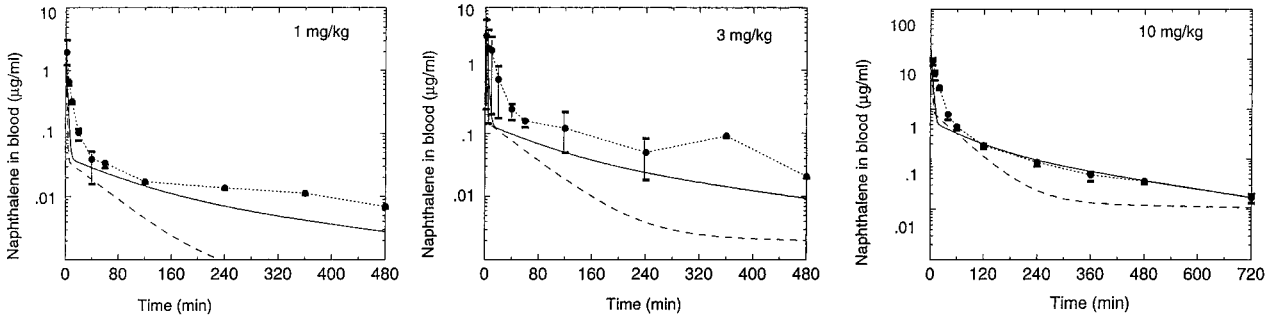

Figure 8. Effect of naphthalene iv dosing (at 1, 3, and 10 mg/kg of body weight) on the time-dependent blood levels of naphthalene in male rats. Data (●) from a NIEHS study (NTP Task No. Chem 00646, 1995) are compared to the model (—) and the Sweeney et al. (1996) model modified for iv dosing (- - -).

Table 6. GSH Depletion: Rat Oral Model

dose (mg/kg)	time (h)	predicted liver GSH	measured liver GSH
200	6.5	17.2	17[a]
500	6.0	10.1	10[b]

[a] Summer et al. (1979). [b] Suga et al. (1966).

contrasts with the only fair comparison to liver GSH after an ip dose (Figure 7). Since the models are identical except for method of dosing, the much more favorable comparison to oral dosing data indicates that either the description of ip uptake may be incorrect, the model is more accurate at longer times, or the experiments are in error. Unfortunately only GSH levels and no other metabolic products (particularly binding levels) have been reported for comparison to rat oral dosing model predictions.

Comparisons were made to data describing the amount of dose excreted as mercapturic acids. The comparison is slightly more uncertain for rats than for mice since experiments report only the total amount of mercapturates excreted rather than the individual GSH conjugates. If the rat excretes the GSH conjugate isomers in the same ratio as the mouse, the same calculations can be performed to estimate percent of dose excreted as mercapturates. The excretion of mercapturic acids by rats has been studied for several oral doses and as a function of time. Model predictions compare well with both (Figure 9).

GSH Levels in Rats and Mice. The models predict significant differences (Figure 10) in the amount of GSH depletion in rats and mice as well as timing of the minima. Lower levels of GSH in the liver of the mouse would allow potentially more reactive metabolites to escape into the circulation and to enter the lung than in the rat.

Sensitivity of Parameters

To assess the sensitivity of the model to values of the various parameters, the effects of individually doubling and halving each parameter were examined (Quick, 1996). The percent differences between normal and new GSH and binding levels were calculated in the lung and liver 4 h after ip dosing with three doses (150, 300, and 450 mg/kg). Thus, in addition to observing the effects of the individual parameters, the effects of dose on the importance of each parameter were also observed.

Overall, the most important parameters to model predictions are $V_{max_{P450}}$ (in the liver for formation of the SR oxide), $V_{max_{EH}}$ (in the liver for metabolism of both the RS and the SR oxides), and C_{li}^{GSH}. These liver V_{max} values and the steady-state concentration of GSH in the liver affected both lung and liver GSH and binding levels considerably (up to 300% difference). Binding levels were significantly affected by the first-order binding rate constants and the K_m values for dihydrodiol formation in the liver (suggesting that dihydrodiol is the primary competing reaction for binding).

The effects of the parameter $V_{max_{P450}}$ (liver, SR oxide) depended strongly on the dose. At the lowest dose tested (150 mg/kg), $V_{max_{P450}}$ (liver, SR oxide) was not particularly significant; however, at the two higher doses, more oxide is produced in the liver than can react there with the normal values of all parameters. Doubling $V_{max_{P450}}$ (liver, RS oxide) intensified the high-dose situation even though $V_{max_{P450}}$ (liver, RS oxide) was not nearly as important. At low doses doubling $V_{max_{P450}}$ (liver, SR oxide) did not produce the same excess of oxides and thus was not as critical to model predictions.

This sensitivity analysis suggests that the composition of the oxides formed from naphthalene metabolism by hepatocytes is important. Also, dosing of cells with the

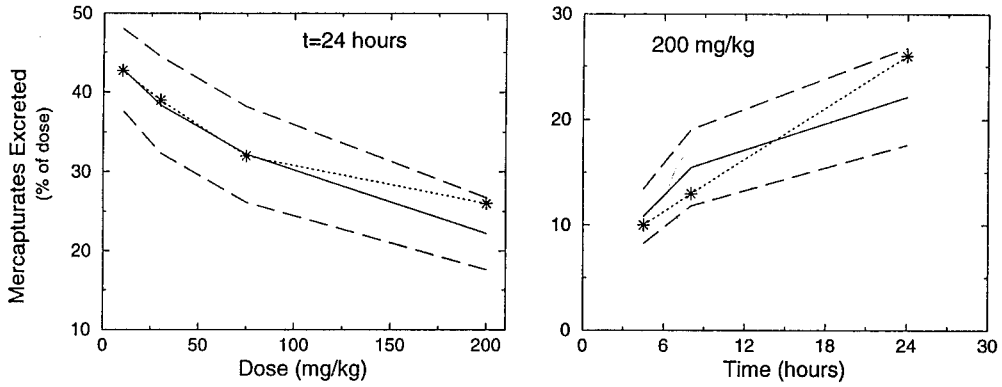

Figure 9. Effect of various naphthalene doses on mercapturates excreted (at 24 h) and on the time-dependent levels of mercapturates excreted at a naphthalene dose of 200 mg/kg in rats. Data (*) from Summer et al. (1979) are compared to the estimated level of excreted mercapturates (—). The prediction is based on averaged values of each naphthalene oxide−GSH conjugate excreted (80% of RS and 62% of SR), and the upper and lower bounds (76−84% of RS and 39−75% for SR) on the estimates are shown (- - -).

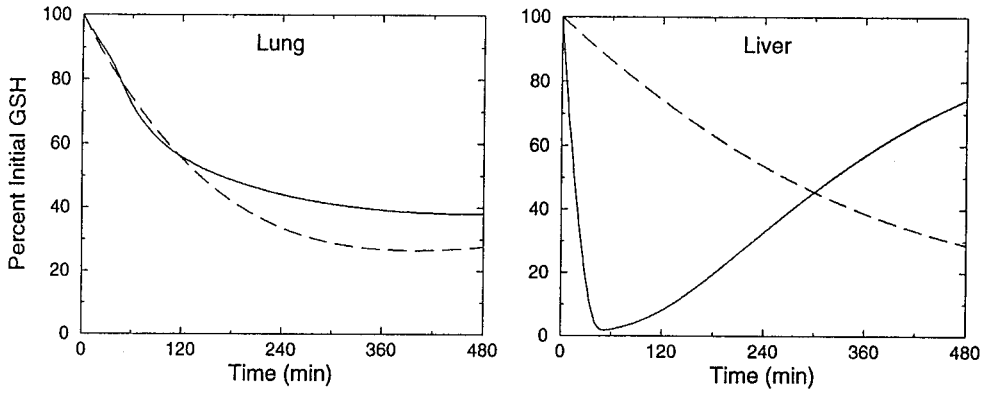

Figure 10. Differences in GSH depletion in the lungs and liver of rats and mice when both are given a 200 mg/kg ip naphthalene dose. The mouse predictions are given as a solid line (—) and rat predictions as a dashed line (- - -).

oxides separately is needed to determine accurately the rates of formation of the secondary metabolites. Accurate determination of the steady-state level of GSH in the mouse liver would also be beneficial. Once these parameters are successfully determined, the sensitivity analysis would need to be reevaluated, since other factors may become important if different values for these other kinetic parameters are placed in the model.

Discussion

Species Comparison. The rat shows much less metabolism than the mouse both in cell fractions and in the animal. While the largest difference is in the values of V_{max} describing the P450 monooxygenases, nearly all the rat enzymes have smaller V_{max} values than the mouse. The lower activity leads not only to less metabolic products but also to slower removal of naphthalene and its products from the animal (Figure 10). A notable model prediction is that mouse lung and liver reach GSH minima at close to the same time after dosing, whereas the rat lung and liver have greatly different GSH minima; this difference could contribute to the more detrimental effects of naphthalene in the mouse. Since the rat lung GSH reserves have been repleted by the time the liver reaches its GSH minimum (when the oxide level in the liver reaches its maximum), the rat lung would be able to form GSH conjugates more readily than in the mouse. Increased GSH would better protect the rat lung from any toxic reactions resulting from high epoxide concentrations.

Model predictions for the makeup of the secondary metabolites may also be a good indicator for determining species susceptibility. At a dose of 200 mg/kg in mice and rats, the model predicts a similar breakdown of the metabolites in both mice and rats (about 60% of the metabolites formed as GSH conjugates, about 40% dihydrodiol, about 0.25% bound to proteins, and a negligible fraction forming naphthol). A drastically different metabolite production occurs in the mouse at a dose of 400 mg/kg. At this higher dose, GSH conjugate makes up only about 40%, dihydrodiol about 60%, and binding and naphthol formation have both tripled (although they are each still an insignificant fraction of the total). In the rat 8 h after a dose of 400 mg/kg, the change is not as significant. The balance among the competing reactions shifts in the mouse model between doses of 200 and 400 mg/kg (as would be expected since the LD_{50} falls between these two doses), and no dominant shift in metabolic pathways occurs in the rat between the same two doses. Even at doses above 800 mg/kg in the rat, little change was observed in metabolite production.

Covalent binding levels of epoxide to proteins in the lung have been suggested as an indicator of toxicity (Warren et al., 1982; Buckpitt and Warren, 1983; Tingle et al., 1993; Wilson et al., 1995). Lung epoxide binding levels at the reported oral and ip LD_{50} values in the mouse were compared and found to be similar. At an ip dose of 380 mg/kg (ip LD_{50}: Shank et al., 1980), the model predicts mouse lung binding at about 0.41 nmol/mg total protein 5 h after dosing; 5 h after an oral dose of 350 mg/kg (oral LD_{50}- Plasterer et al., 1985), the predicted binding is about 0.49 nmol/mg of total protein. Assuming that covalent binding of the epoxides is the cause for toxicity, the similar binding levels suggest that there may be a threshold for epoxide covalent binding levels (about

0.45 nmol/mg of total protein (tp)) which might be toxic for the mouse. This analysis ignores the possible role for the quinones formed from naphthol (Wilson et al., 1996; Zheng et al., 1997), but this approximation can be justified by the low predicted level of naphthol.

For the rat, an oral LD_{50} has been reported (2200−2400 mg/kg: Gaines et al., 1969) that is significantly higher than an approximate ip LD_{50} (1600 mg/kg: Plopper et al., 1992). At both 2300 mg/kg 5 h after oral dosing and at 1600 mg/kg after ip dosing, predicted rat lung binding levels are both about 0.17 nmol/mg of tp. This significantly lower binding in the rat lung agrees with the lack of pulmonary toxicity observed in rats. Although mice die from the harmful effects of naphthalene to their lung cells, rats die from liver enzyme failure (Germansky and Jamall, 1988). Thus a lower binding level in the rat lung would be expected.

Although almost all of the rat enzymes were determined to have lower activity than mouse enzymes, rat lung epoxide hydrolase (EH) is the exception. Higher EH activity in rat lung may help protect the rat lung. Of course the approximately 3 times lower formation of epoxides (P450 activity) in rat lung and liver would likely contribute more to the reduced effects of naphthalene in rats. Rats and mice appear to have similar rates of formation of all oxide metabolites except GSH conjugates and lung dihydrodiols. Lower GST activity in rats and similar binding rates might suggest an increased risk for rats; however, the low GST activity actually prevents GSH levels from dropping to low levels where binding (or any other competing toxic reaction) would be favored.

These differences in rate constants concur with the data on excretion products. Primary excretion products in mice include metabolites of naphthol, dihydrodiol, and GSH conjugates. Rats, on the other hand, primarily excrete the naphthol and dihydrodiol products. The lower percentage of GSH conjugate metabolites in rat urine follows from the lower GST activity with similar rates for other metabolites. One data point describing excretion by mice following 100 mg/kg ip naphthalene exposure (Stillwell et al., 1982) may be compared to excretion by rats after the same dose (Horning et al., 1980). A much higher percentage of the dose is excreted by the mouse (approximately 65% of the dose excreted in 24 h versus about 25% excreted by the rat). According to the model, higher P450 activity in mice is the largest contributor to the faster excretion.

Buckpitt and Franklin (1989) suggest that the species-specific effects may be due to the stereoselectivity of oxide formation. Only the mouse lung generates more *RS* oxide than *SR* oxide; thus it is possible that increased *RS* oxide formation in the mouse lung contributes to the cytotoxicity observed there. However, at high doses, the models predict a drop in the *RS*/*SR* ratio in the mouse lung, mouse liver, and rat liver. Oddly, only the rat lung is predicted to have an increasing *RS*/*SR* ratio with increasing dose. Thus the model suggests that the relative formation of *RS* and *SR* oxide is probably not a significant factor in toxicity. The model results favor an explanation where differences in secondary enzyme activities and consequently differences in GSH levels when epoxide concentrations are high result in increased vulnerability of mouse lung tissue.

Ultimately, a PBPK model similar to the ones written for mice and rats could be written to examine the metabolism of naphthalene by humans. Studies have been performed with human lung and liver microsomes although not to the extent necessary to determine kinetic parameters for a human naphthalene PBPK model. Preliminary experiments with human liver microsomes (Tingle et al., 1993) show that human liver microsomes have considerably lower P450 activity and considerably higher EH activity than mouse and rat liver microsomes. Since rat liver microsomes have lower P450 and higher EH activity than mouse liver microsomes, the further reduction in primary metabolite forming enzyme (P450) activity and increase in nontoxic secondary metabolite forming enzyme (EH) activity would suggest that humans are at an even lower risk of naphthalene toxicity than rats. Experiments with human lung microsomes also suggest lower capacity of human enzymes (Buckpitt and Bahnson, 1986).

Model Limitations: Biochemical Parameters. The mouse and rat models make reasonable to excellent predictions for a wide range of data. Such favorable comparison, however, does not imply that the models are without weaknesses.

This model was undertaken with the intent of developing an animal model purely from in vitro data. The primary advantage of such an approach is that independently estimated parameters provide a better test of the proposed biochemical mechanism in the mathematical model than if in vivo data were used to determine the kinetic parameters. Also in vitro experiments may be designed to isolate a reaction to prevent interfering influences, such as membrane transport, blood flow, and competing reactions. The applicability of in vitro experiments to the animal has been questioned. In determination of Michaelis constants, the concentration determined to be limiting in an in vitro system may not be equivalent in vivo due to compartmentation and mass transfer limitations. The in vitro concentration may be related to the in vivo concentration through a series of partition coefficients (buffer:air, blood:air, and tissue:air) as suggested by Csanády et al. (1994), or Michaelis constants may be used unchanged from cell fraction incubations as suggested by Lin et al. (1982). Another concern with using in vitro data to predict in vivo activity is that the enzyme may adopt a different conformation in vitro that may affect its kinetic properties.

To find the most representative biochemical parameters, an approach was used to determine biochemical rate constants which combined knowledge gained from cell fraction and primary cell incubations. In this method the cell served as a bridge between the cell fractions and the animal tissues. Parameters fit to cell fraction experiments (where reactions can be more easily isolated and where membrane transport is presumably not significant) were modified to fit primary cell incubations. Most of the biochemical rate constants were determined for the mouse model using this procedure, but no data have been published for rat lung and liver cells. Thus, for the rat model, biochemical parameters were based solely on cell fraction incubations. It should be noted, however, that the rat model is equally as accurate as the mouse model. The shortage of rat cell fraction data and absence of rat cell data complicates parameter determination (resulting in nonunique parameters). Thus, although the rat PBPK model predictions are accurate, the additional step of fitting parameters to primary cells as done with the mouse model (rather than simply fitting parameters to cell fractions) would provide a check on cell fraction data and probably result in more representative parameters for predicting in vivo metabolism.

One rate constant could not be fit with the above approach. While the rate of naphthalene oxide binding fitted with the cell model should apply to the animal, the best values of epoxide−protein binding rates for matching

animal data were about half the rates determined to fit the cell data. The use of different binding rates in the cell and animal models implies that other factors affect the apparent binding. The different modeling approaches for the cells and organs (cells and extracellular medium as separate compartments versus a well-mixed organ compartment) affect the level of epoxide available for binding. In addition to these modeling differences, the system differences (for example, flow versus static incubation) probably affect the apparent binding rates. More experiments identifying the proteins susceptible to binding with naphthalene oxides (like in Cho et al., 1994b) are necessary to eliminate these adjustable binding rates. Further, the complications from nonenzymatic rearrangement to naphthol and subsequent reaction to quinones need to be considered, particularly as these reactions may differ considerably in in vitro systems with large fluid to cell volumes from that in vivo. The final binding rates used in the PBPK model were based on in vivo data. Although the use of an adjustable parameter weakens the model, there were no accurate independent estimates for the binding rates based solely on the in vitro cell fraction and cell culture data.

Important to the GSH status of the tissues, the rate of conjugation in the tissues significantly affects comparison to all of the data. The assumption of "effective" cytosolic protein (smaller than the actual amount) is critical to the rate of conjugation of naphthalene oxide and GSH since the amount of cytosolic protein is multiplied by the V_{max} determined from the cell and cell fraction experiments. Experiments indicate that, above certain ratios of cytosolic protein to microsomal protein, the amount of products formed plateaus (Buckpitt et al., 1984). The model includes this empirical observation, but its underlying meaning is unclear (although localization of GST is possible). If parameter sets were determined from experiments with different cytosolic to microsomal protein ratios, then a more accurate rate of conjugate formation could be obtained and artificially limiting the cytosolic protein content would not be necessary.

Model Limitations: Model Structure. One questionable aspect of the model structure is the use of partition coefficients describing mass transfer between the organs and blood. Naphthalene and naphthalene oxide transfer between the blood and tissues have not been examined to the extent necessary to determine if transport is diffusion-limited or whether instantaneous equilibrium (as was assumed in this model) is achieved. Even assuming that naphthalene and its oxide reach equilibrium between the blood and tissues, the determination of partition coefficients for this model involves some uncertainty. PCs were estimated using equations relating tissue:blood PCs to the partitioning of the compound between oil and air and between water and air (Abraham et al., 1985; Fiserova-Bergerova and Diaz, 1986). Naphthalene is not as volatile as many of the compounds included in determination of the equations and is much less water-soluble than most. Also an oil: air partition coefficient for naphthalene has not been reported; thus an octanol:water PC was used in conjunction with the water:air PC to estimate an oil:air PC prior to estimating the tissue:blood PCs. Experiments need to be conducted to determine whether naphthalene and naphthalene oxide transport are diffusion- or flow-limited. In either case, direct measurement of the parameters describing the transport (diffusion rates or tissue:blood PCs) are needed.

Although the kinetic description could be the cause for the poor match between predicted and actual lung naphthalene oxide binding levels at high doses (Figure 3), it is possible that the description of mass transfer affects the predicted binding in the lung. Perhaps more epoxide leaves the liver at high doses than is allowed by simple partitioning; for example, an active transport system could be in place to export the oxides from the liver. Another possibility for the poor agreement to data is an inadequate description of the lung structure (ignoring structural and cell diversity). Clara cells make up only 5% of the lung cell population, yet they are the basis for kinetic parameters for the mouse lung compartment.

Recommendations

Although this PBPK model is fairly successful at simulating the available in vivo data using all but one parameter estimated from in vitro experiments, many additional experiments would be helpful for determining better values of kinetic parameters for future PBPK models for naphthalene and related compounds.

Experiments where cell fractions (microsomal and cytosolic) from mice, rats, and humans are exposed to a wide range of naphthalene oxide and glutathione (GSH) levels are needed. The cytosolic fraction is preferred for these experiments over purified GST (glutathione-S-transferase) due to the simplified scale-up from the cell fraction model to the cell or animal models. Even more importantly, primary cells need to be studied over a wider range of naphthalene and naphthalene oxide concentrations. The rates of naphthalene oxide binding to proteins need to be measured, and the proteins susceptible to binding by naphthalene oxide need to be identified (extension of Cho et al., 1994b). The amount of these susceptible proteins in the tissues needs to be quantified, and the rate of covalent binding to the proteins in their native state needs to be determined. Also, the in vivo importance of naphthol formation of quinones and their role in toxicity needs to be clarified.

In addition to further analysis of kinetic mechanisms, the mechanisms of mass transfer for naphthalene, naphthalene oxide, and the GSH conjugates should be studied. Measurement of intracellular and extracellular concentrations of these components in cell incubations as well as measurements of organ and flowing medium concentrations in isolated perfused organ experiments should indicate the most prominent mechanisms of mass transfer.

Conclusions

Naphthalene metabolism is predicted well with this PBPK model. Comparison to reported GSH and binding levels, percent of dose excreted as mercapturic acids, and naphthalene blood concentrations in the mouse and rat is favorable. Since in vitro parameters only (except epoxide binding) were used, the ability to predict whole animal response without fitting to animal data suggests that the mechanisms incorporated into the model may be a valid representation of biochemical mechanisms. A strategy combining cell fraction data and primary culture data was useful for naphthalene and may be generally applicable.

Differences in mouse and rat model predictions suggest that the cause for the species differences is due to the values of the kinetic parameters. Switching the kinetic parameters of the rat and mouse models results in a rat model that behaves like the mouse model and a mouse model that behaves like the original rat model. The mouse model shows large surges in naphthalene oxide concentrations near the LD_{50}, while no such surge is observed in the rat at any dose. The surge in naphthalene

oxide concentration in the mouse model occurs at the same time as the mouse lung and liver reach their GSH minima. Contrary to the mouse, the rat lung and liver GSH minima do not occur simultaneously, thus each organ is protected from any circulating oxides.

Notation

V_{max_J} maximum reaction rate by enzyme J (for J = P450 or EH, units are nmol/mg of mp/min; for J = GST, units are nmol/mg of cp/min), Vmax values are specific to each enantiomer in each tissue

$K_{m^y_J}$ Michaelis constant for component y in rate expression for enzyme J (μM), K_m values are specific to each enantiomer in each tissue

$D1_x$ constant in denominator of conjugation rate expression in compartment x assuming ordered conjugation (μM^2)

$D2_x$ constant in denominator of conjugation rate expression in compartment x (μM), multiplied by the naphthalene oxide concentration

$D3_x$ constant in denominator of conjugation rate expression in compartment $_x$ (μM), multiplied by the GSH concentration

y_{noh} rate constant for rearrangement of naphthalene oxide to 1-naphthol (1/min)

sl_{noh} constant relating naphthol formation rate to protein content (mL/g of total protein)

k_x^{GS} zero-order rate of GSH synthesis (μM GSH/min)

k_x^{GD} first-order rate of GSH degradation (1/min)

y component: naphthalene (N), glutathione (GSH), RS or SR naphthalene oxide (NO), RS + SR naphthalene oxide (NOt), dihydrodiol (D)

J enzyme: P450 (cytochrome P450 monooxygenases), EH (epoxide hydrolase), GST (glutathione-S-transferase)

mp, cp, tp microsomal, cytosolic, and total protein, respectively, in the previous definitions

Specific to Cell Model

CC_x^y concentration of component y in type x cells (μM)

CM_x^y concentration of component y in medium incubated with type x cells (μM)

VC_x volume of type x cells in the incubation (mL)

VM_x volume of medium in the incubation with type x cells (mL)

P_x cell: medium partition coefficient (PC) (μM in type x cells/μM in surrounding medium)

TP_x mg total protein in type x cells or in medium (x = m) in the incubation

MP_x mg of microsomal protein in the incubation with type x cells

CP_x mg of assumed active cytosolic protein in the incubation with type x cells

kb_x binding rate (nmol/mg of tp/μM naphthalene oxide/min)

x lu (lung) or li (liver)

Specific to PBPK Model

C_x^y concentration of component y in compartment x (μM)

V_x volume of compartment x (mL)

Q_x volumetric flow rate of blood through compartment x (mL/min)

Q_v volumetric flow rate of air through the lung (mL/min)

P_x compartment: blood partition coefficient (PC) in compartment x (μM in compartment x/μM in exiting blood)

P_{fn}, P_{fno} fat: blood PCs for naphthalene and naphthalene oxide

P_{air} blood: air PC for exhalation of naphthalene from the lung

MP_x mg of microsomal protein/ mL of compartment x

CP_x mg of assumed active cytosolic protein/mL of compartment x (limiting ratio of cytosolic protein to microsomal protein observed in vitro; Buckpitt et al., 1984)

TP_x g of total protein/mL of compartment x

k_{b_x} rate constant for covalent binding of naphthalene oxide to proteins in compartment x (nmol/g of tp/μM naphthalene oxide/min)

k_{ip} rate of ip uptake (nmol/min)

k_{up} rate of oral uptake (1/min)

x compartment: blood (bl), lung (lu), liver (li), f (fat), r (richly perfused tissues), p (poorly perfused tissues), ab (arterial blood), vb (venous blood), air (air in chamber holding the animal)

Acknowledgment

We thank Alan Buckpitt and Dexter Morin (UC Davis) for clarifying the details of their experiments and thank Amyl Ghanem (currently at University of Maine) and Lisa Sweeney (Chemical Industry Institute for Toxicology) for many helpful discussions. D.J.Q. was supported, in part, by the Fred Rhodes and Henry L. Mattin scholarships. Our efforts have been supported, in part, by a gift from DuPont and the Cornell Center for Advanced Technology, which is sponsored by the New York State Science and Technology Foundation.

Appendix

PBPK Model Equations.

Lung Compartment: Naphthalene (N)

$$\frac{dC_{lu}^N}{dt} = \frac{Q_{lu}}{V_{lu}}\left(C_{vb}^N - \frac{C_{lu}^N}{P_{lu}}\right) - \frac{V_{max_{P450}} C_{lu}^N}{K_{m_{P450}^N} + C_{lu}^N} MP_{lu} - \frac{Q_V}{V_{air}} \frac{C_{lu}^N}{P_{lu} P_{air}} \quad (1)$$

Lung Compartment: RS or SR Naphthalene Oxide (NO)

$$\frac{dC_{lu}^{NO}}{dt} = \frac{Q_{lu}}{V_{lu}}\left(C_{vb}^{NO} - \frac{C_{lu}^{NO}}{P_{lu}}\right) + \frac{V_{max_{P450}} C_{lu}^N}{K_{m_{P450}^N} + C_{lu}^N} MP_{lu} - \frac{V_{max_{EH}} C_{lu}^{NO}}{K_{m_{EH}^{NO}} + C_{lu}^{NO}} MP_{lu} - k_{b_{lu}} C_{lu}^{NO} TP_{lu} - \frac{V_{max_{GST}} C_{lu}^{NO} C_{lu}^{GSH}}{D1_{lu} + D2_{lu} C_{lu}^{NO} + D3_{lu} C_{lu}^{GSH} + C_{lu}^{NO} C_{lu}^{GSH}} \times CP_{lu} - y_{noh} \exp(-sl_{noh} TP_{lu}) C_{lu}^{NO} \quad (2)$$

Liver Compartment: Naphthalene (N)

$$\frac{dC_{li}^N}{dt} = \frac{Q_{li}}{V_{li}}\left(C_{ab}^N + Dose - \frac{C_{li}^N}{P_{li}}\right) - \frac{V_{max_{P450}} C_{li}^N}{K_{m_{P450}^N} + C_{li}^N} MP_{li} \quad (3)$$

Liver Compartment: RS or SR Naphthalene Oxide (NO)

$$\frac{dC_{li}^{NO}}{dt} = \frac{Q_{li}}{V_{li}}\left(C_{ab}^{NO} - \frac{C_{li}^{NO}}{P_{li}}\right) + \frac{V_{max_{P450}} C_{li}^{N}}{K_{m_{P450}^{N}} + C_{li}^{N}} MP_{li} - \frac{V_{max_{EH}} C_{li}^{NO}}{K_{m_{EH}^{NO}} + C_{li}^{NO}} MP_{li} - k_{b_{li}} C_{li}^{NO} TP_{li} - \frac{V_{max_{GST}} C_{li}^{NO} C_{li}^{GSH}}{D1_{li} + D2_{li} C_{li}^{NO} + D3_{li} C_{li}^{GSH} + C_{li}^{NO} C_{li}^{GSH}} \times CP_{li} - y_{noh} \exp(-sl_{noh} TP_{li}) C_{li}^{NO} \quad (4)$$

The term "Dose" in the above liver compartment naphthalene balance applies to intraperitoneal (ip) and oral (po) dosing and indicates that the dose first enters the circulation through the liver. For ip dosing, Dose = k_{ip}/Q_{li}. For oral (po) dosing, Dose = k_{up}(oral dose) $\exp^{(-k_{up}t)}/Q_{li}$.

All Other Organ Compartments (x = f, r, or p): Naphthalene (N)

$$\frac{dC_x^N}{dt} = \frac{Q_x}{V_x}\left(C_{ab}^{N} - \frac{C_x^N}{P_x}\right) \quad (5)$$

All Other Organ Compartments: RS or SR Naphthalene Oxide (NO)

$$\frac{dC_x^{NO}}{dt} = \frac{Q_x}{V_x}\left(C_{ab}^{NO} - \frac{C_x^{NO}}{P_x}\right) - y_{noh} \exp(-sl_{noh} TP_x) \times C_x^{NO} - k_{b_x} C_x^{NO} TP_x \quad (6)$$

Arterial Blood Compartment: Naphthalene (N)

$$\frac{dC_{ab}^N}{dt} = \frac{Q_c}{V_{ab}}\left(\frac{C_{lu}^N}{P_{lu}} - C_{ab}^N\right) \quad (7)$$

Arterial Blood Compartment: RS or SR Naphthalene Oxide (NO)

$$\frac{dC_{ab}^{NO}}{dt} = \frac{Q_c}{V_{ab}}\left(\frac{C_{lu}^{NO}}{P_{lu}} - C_{ab}^{NO}\right) - y_{noh} \exp(-sl_{noh} TP_{bl}) \times C_{ab}^{NO} - k_{b_{bl}} C_{ab}^{NO} TP_{bl} \quad (8)$$

Venous Blood Compartment: Naphthalene (N)

$$\frac{dC_{vb}^N}{dt} = \frac{1}{V_{vb}}\left(\frac{Q_{li} C_{li}^N}{P_{li}} + \frac{Q_f C_f^N}{P_{fn}} + \frac{Q_r C_r^N}{P_r} + \frac{Q_p C_p^N}{P_p} - Q_c C_{vb}^N\right) \quad (9)$$

Venous Blood Compartment: RS or SR Naphthalene Oxide (NO)

$$\frac{dC_{vb}^{NO}}{dt} = \frac{1}{V_{vb}}\left(\frac{Q_{li} C_{li}^{NO}}{P_{li}} + \frac{Q_f C_f^{NO}}{P_{fno}} + \frac{Q_r C_r^{NO}}{P_r} + \frac{Q_p C_p^N}{P_p} - Q_c C_{vb}^{NO}\right) - k_{b_{bl}} C_{vb}^{NO} TP_{bl} - y_{noh} \exp(-sl_{noh} TP_{bl}) C_{vb}^{NO} \quad (10)$$

Glutathione Balance (x = li or lu, C_x^{NOt} refers to RS nap. oxide + SR nap. oxide)

$$\frac{dC_x^{GSH}}{dt} = \frac{k_x^{GS}}{V_x} - k_x^{GD} C_x^{GSH} - \frac{V_{max_{GST}} C_x^{NOt} C_x^{GSH}}{D1_x + D2_x C_x^{NOt} + D3_x C_x^{GSH} + C_x^{NOt} C_x^{GSH}} \quad (11)$$

Air Chamber: For Exhaled Naphthalene

$$\frac{dC_{air}^N}{dt} = \frac{Q_v}{V_{lu}}\left(\frac{C_{lu}{}^N}{P_{lu} P_{air}}\right) \quad (12)$$

Inhalation. When exposed to naphthalene in the air, the dose is modeled as first entering the lung; thus, the mass balances for naphthalene in the lung, liver, and air chambers are different than when dosing ip or orally.

Lung Compartment

$$\frac{dC_{lu}^N}{dt} = \frac{Q_{lu}}{V_{lu}}\left(C_{vb}^N - \frac{C_{lu}^N}{P_{lu}}\right) - \frac{V_{max_{P450}} C_{lu}^N}{K_{m_{P450}^N} + C_{lu}^N} MP_{lu} + \frac{Q_v}{V_{lu}}\left(C_{air}^N - \frac{C_{lu}^N}{P_{lu} P_{air}}\right) \quad (13)$$

Liver Compartment

$$\frac{dC_{li}^N}{dt} = \frac{Q_{li}}{V_{li}}\left(C_{ab}^N - \frac{C_{li}^N}{P_{li}}\right) - \frac{V_{max_{P450}} C_{li}^N}{K_{m_{P450}^N} + C_{li}^N} MP_{li} \quad (14)$$

Air Chamber

$$\frac{dC_{air}^N}{dt} = \frac{Q_v}{V_{lu}}\left(\frac{C_{lu}^N}{P_{lu} P_{air}} - C_{air}^N\right) \quad (15)$$

Intravenous Dosing. When dosing intravenously, the dose first enters the venous blood compartment; thus, the mass balances for the liver and venous blood are different than when dosing ip or orally. k_{iv} = rate of iv uptake (nmol/min).

Liver Compartment

$$\frac{dC_{li}^N}{dt} = \frac{Q_{li}}{V_{li}}\left(C_{ab}^N - \frac{C_{li}^N}{P_{li}}\right) - \frac{V_{max_{P450}} C_{li}^N}{K_{m_{P450}^N} + C_{li}^N} MP_{li} \quad (16)$$

Venous Blood Compartment

$$\frac{dC_{vb}^N}{dt} = \frac{1}{V_{vb}}\left(\frac{Q_{li} C_{li}^N}{P_{li}} + \frac{Q_f C_f^N}{P_{fn}} + \frac{Q_r C_r^N}{P_r} + \frac{Q_p C_p^N}{P_p} - Q_c C_{vb}^N\right) + \frac{k_{iv}}{V_{vb}} \quad (17)$$

Cell Model Equations.

Naphthalene in the Cells

$$\frac{dCC_x^N}{dt} = \frac{1}{\left(VC_x + \frac{VM_x}{P_x}\right)}\left(-\frac{V_{max_{P450}} CC_x^N}{K_{m_{P450}^N} + CC_x^N} MP_x\right) \quad (18)$$

RS or SR Naphthalene Oxide (NO) in the Cells

$$\frac{dCC_x^{NO}}{dt} = \frac{1}{\left(VC_x + \frac{VM_x}{P_x}\right)}\left(\frac{V_{max_{P450}} CC_x^N}{K_{m_{P450}^N} + CC_x^N} MP_x - \frac{V_{max_{EH}} CC_x^{NO}}{K_{m_{EH}^{NO}} + CC_x^{NO}} MP_x + k_{b_x} CM_x^{NO} TP_m\right) - \frac{1}{\left(VC_x + \frac{VM_x}{P_x}\right)} \times \left(\frac{V_{max_{GST}} CC_x^{NO} CC_x^{GSH}}{D1_x + D2_x CC_x^{NO} + D3_x CC_x^{GSH} + CC_x^{NO} CC_x^{GSH}} CP_x\right) - \frac{1}{\left(VC_x + \frac{VM_x}{P_x}\right)}\left(y_{noh} \exp\left(-sl_{noh} \frac{TP_m}{1000 VM_x}\right) CM_x^{NO} \times (P_x VC_x + VM_x)\right) - \frac{1}{\left(VC_x + \frac{VM_x}{P_x}\right)}(k_{b_x} CC_x^{NO} TP_x) - y_{noh} \exp\left(-sl_{noh} \frac{TP_x}{1000 VC_x}\right) CC_x^{NO} \quad (19)$$

Glutathione in the Cells

$$\frac{dCC_x^{GSH}}{dt} = k_x^{GS} - k_x^{GD} CC_x^{GSH} - \frac{V_{max_{GST}} CC_x^{NOt} CC_x^{GSH}}{D1_x + D2_x CC_x^{NOt} + D3_x CC_x^{GSH} + CC_x^{NOt} CC_x^{GSH}} \frac{CP_x}{VC_x} \quad (20)$$

Naphthalene (N) in the Medium

$$\frac{dCM_x^N}{dt} = \frac{1}{(P_x VC_x + VM_x)}\left(-\frac{V_{max_{P450}} CC_x^N}{K_{m_{P450}^N} + CC_x^N} MP_x\right) \quad (21)$$

RS or SR Naphthalene Oxide (NO) in the Medium

$$\frac{dCM_x^{NO}}{dt} = \frac{1}{(P_x VC_x + VM_x)}\left(\frac{V_{max_{P450}} CC_x^N}{K_{m_{P450}^N} + CC_x^N} MP_x - \frac{V_{max_{EH}} CC_x^{NO}}{K_{m_{EH}^{NO}} + CC_x^{NO}} MP_x + k_{b_x} CM_x^{NO} TP_m\right) - \frac{1}{(P_x VC_x + VM_x)} \times \left(\frac{V_{max_{GST}} CC_x^{NO} CC_x^{GSH}}{D1_x + D2_x CC_x^{NO} + D3_x CC_x^{GSH} + CC_x^{NO} CC_x^{GSH}} CP_x\right) - \frac{1}{(P_x VC_x + VM_x)}\left(y_{noh} \exp\left(-sl_{noh} \frac{TP_x}{1000 VC_x}\right) CC_x^{NO} \times \left(VC_x + \frac{VM_x}{P_x}\right)\right) - \frac{1}{(P_x VC_x + VM_x)}(k_{b_x} CC_x^{NO} TP_x) - y_{noh} \times \exp\left(-sl_{noh} \frac{TP_m}{1000 VM_x}\right) CM_x^{NO} \quad (22)$$

References and Notes

Abraham, M.; Kamlet, M.; Taft, R.; Doherty, R.; Weathersby, P. Solubility properties in polymers and biological media. 2. The correlation and prediction of the solubilites of nonelectrolytes in biological tissues and fluids. *J. Med. Chem.* **1985**, *28*, 865−870.

Andersen, M.; Clewell, H., III; Gargas, M.; Smith, F.; Reitz, R. Physiologically based pharmacokinetics and the risk assessment process for methylene chloride. *Toxicol. Appl. Pharm.* **1987**, *87*, 185−205.

Buckpitt, A.; Bahnson, L. Naphthalene metabolism by human lung microsomal enzymes. *Toxicology* **1986**, *41*, 333−341.

Buckpitt, A.; Franklin, R. Relationship of naphthalene and 2-methyl-naphthalene metabolism to pulmonary bronchiolar epithelial cell necrosis. *Pharmacol. Ther.* **1989**, *41*, 393−410.

Buckpitt, A.; Warren, D. Evidence for hepatic formation, export and covalent binding of reactive naphthalene metabolites in extrahepatic tissues *in vivo*. *J. Pharm. Exp. Ther.* **1983**, *225*, 8−15.

Buckpitt, A.; Bahnson, L.; Franklin, R. Hepatic and pulmonary microsomal metabolism of naphthalene to glutathione adducts: factors affecting the relative rates of conjugate formation. *J. Pharm. Exp. Ther.* **1984**, *231*, 291−300.

Buckpitt, A. R.; Bahnson, L. S.; Franklin, R. B. Evidence that 1-naphthol is not an obligate intermediate in the covalent binding and pulmonary bronchiolar necrosis by naphthalene. *Biochem. Biophys. Res. Common.* **1985**, *126*, 1097−1103.

Buckpitt, A.; Buonarati, M.; Bahnson-Avey, L.; Chang, A.; Morin, D.; Plopper, C. Relationship of cytochrome P450 activity to Clara cell cytotoxicity. II. Comparison of stereoselectivity of naphthalene epoxidation in lung and nasal mucosa of mouse, hamster, rat and rhesus monkey. *J. Pharmacol. Exp. Ther.* **1992**, *261*, 364−372.

Buckpitt, A.; Chang, A.; Weir, A.; Van Winkle, L.; Duan, X.; Philpot, R.; Plopper, C. Relationship of cytochrome P450 activity to Clara cell cytotoxicity. IV. Metabolism of naphthalene and naphthalene oxide in microdissected airways from mice, rats, and hamsters. *Mol. Pharm.* **1995**, *47*, 74−81.

Buonarati, M.; Morin, D.; Plopper, C.; Buckpitt, A. Glutathione depletion and cytotoxicity by naphthalene 1,2-oxide in isolated hepatocytes. *Chem.-Biol. Interact.* **1989**, *71*, 147−165.

Buonarati, M.; Jones, A.; Buckpitt, A. In vivo metabolism of isomeric naphthalene oxide glutathione conjugates. *Drug Metab. Dispos.* **1990**, *18*, 183−189.

Chen, K.-C.; Dorough, H. W. Glutathione and mercapturic acid conjugations in the metabolism of naphthalene and 1-naphthyl-*N*-methylcarbamate (carbaryl). *Drug Chem. Toxicol.* **1979**, *2*, 331−354.

Chichester, C.; Buckpitt, A.; Chang, A.; Plopper, C. Metabolism and cytotoxicity of naphthalene and its metabolites in isolated murine Clara cells. *Mol. Pharmacol.* **1994**, *45*, 664−672.

Cho, M.; Jedrychowski, R.; Hammock, B.; Buckpitt, A. Reactive naphthalene metabolite binding to hemoglobin and albumin. *Fundam. Appl. Toxicol.* **1994a**, *22*, 26−33.

Cho, M.; Chichester, C.; Morin, D.; Plopper, C.; Buckpitt, A. Covalent interactions of reactive naphthalene metabolites with proteins. *J. Pharm. Exp. Ther.* **1994b**, *269*, 881−889.

CRC Handbook of Chemistry and Physics, 71st ed.; CRC Press: Boca Raton, FL, 1990; pp 16-25−16-27.

Crispens, C. *Handbook on the Laboratory Mouse*; Thomas Publishing: Sprigfield, IL, 1975.

Crosfill, M.; Widdicombe, J. Physical characteristics of the chest and lungs and the work of breathing in different mammalian species. *J. Physiol.* **1961**, *158*, 1−14.

Csanády, G.; Mendrala, A.; Nolan, R.; Filser, J. A physiologic pharmacokinetic model for styrene and styrene-7,8-oxide in mouse, rat and man. *Arch. Toxicol.* **1994**, *68*, 143−157.

D'Souza, R.; Francis, W.; Andersen, M. Physiological model for tissue glutathione depletion and increased resynthesis after ethylene dichloride exposure. *J. Pharmacol. Exp. Ther.* **1988**, *245*, 563−568.

Duck, F. A. *Physical Properties of Tissue*; Academic Press: San Diego, CA, 1990.

Fanucchi, M. V.; Murphy, M. E.; Buckpitt, A. R.; Philot, R. W.; Plopper, C. G. Pulmonary cytochrome P450 monooxygenase and Clara Cell differentiation. *Am. J. Respir. Cell Mol. Biol.* **1997**, *17*, 302−314.

Fiserova-Bergerova, V.; Diaz, M. Determination and prediction of tissue-gas partition coefficients. *Int. Arch. Occup. Environ. Health* **1986**, *58*, 75−87.

Frederick, C.; Potter, D.; Chang-Mateu, M; Andersen, M. A physiologically based pharmacokinetic and pharmacodynamic model to describe the oral dosing of rats with ethyl acrylate and its implications for risk assessment. *Toxicol. Appl. Pharm*. **1992**, *114*, 246−260.

Gaines, T. B. Acute toxicity of pesticides. *Toxicol. Appl. Pharm*. **1969**, *14*, 515−534.

Gearhart, J.; Jepson, G.; Clewell, H., III; Andersen, M.; Conolly, R. Physiologically based pharmacokinetic model for the inhibition of acetylcholinesterase by diisoproplylfluorophosphate. *Toxicol. Appl. Pharm*. **1990**, *106*, 295−310.

Germansky, M.; Jamall, I. S. Organ-specific effects of naphthalene on tissue peroxidation, glutathione peroxidases and superoxide dismutase in the rat. *Arch. Toxicol.* **1988**, *61*, 480−483.

Griffith, O.; Meister, A. Glutathione: interorgan translocation, turnover and metabolism. *Proc. Natl. Acad. Sci. U.S.A.* **1979**, *76*, 5606−5610.

Haies, D.; Gil, J.; Weibel, E. Morphometric study of rat lung cells I. Numerical and dimensional characteristics of parenchymal cell population. *Am. Rev. Respir. Dis.* **1981**, *123*, 533−541.

Hansch, C.; Leo, A. *Substituent Constants for Correlation Analysis in Chemistry and Biology*; J. Wiley and Sons: New York, 1979.

Horning, M.; Stillwell, W.; Griffin, G.; Tsang, W.-S. Epoxide intermediates in the metabolism of naphthalene by the rat. *Drug Metab. Disp.* **1980**, *8*, 404−414.

Johanneson, K.; DePierre, J.; Bergstrand, A.; Dallner, G.; Ernster, L. Preparation and characterization of total, rough and smooth microsomes from the lung of control and methylcholanthrene treated rats. *Biochim. Biophys. Acta* **1977**, *496*, 115−135.

Kanekal, S.; Plopper, C.; Morin, D.; Buckpitt, A. Metabolism and cytotoxicity of naphthalene oxide in the isolated perfused mouse lung. *J. Pharmacol. Exp. Ther.* **1990**, *256*, 391−401.

Kanekal, S.; Plopper, C.; Morin, D.; Buckpitt, A. Metabolism and cytotoxicity of naphthalene oxide in the isolated perfused mouse lung. *J. Pharmacol. Exp. Ther.* **1991**, *256*, 391−401.

Knox, W. E. *Enzyme Patterns in Fetal, Adult, and Neoplastic Rat Tissues*; S. Karger Publishers. Basel, Switzerland, 1972; pp 256−268.

Lin, J.; Sugiyama, Y.; Awazu, S.; Hanano, M. Physiological pharmacokinetics of ethoxybenzamide based on biochemical data obtained *in vitro* as well as on physiological data. *J. Pharmacokinet. Biopharm*. **1982**, *10*, 649−661.

Medinsky, M.; Leavens, T.; Gargas, M.; Bond, J. In vivo metabolism of butadiene by mice and rats: a comparison of physiological model predictions and experimental data. *Carcinogenesis* **1994**, *15*, 1329−1340.

NTP Task No. Chem00646. Routine Biological Sample Analysis for Naphthalene in Rodent Blood, National Toxicology Program, April 19, 1995.

O'Brien, K.; Smith, L.; Cohen, G. Differences in naphthalene-induced toxicity in the mouse and rat. *Chem.-Biol. Interact.* **1985**, *55*, 109−122.

Plasterer, M.; Bradshaw, W.; Booth, G.; Carter, M.; Schuler, R.; Hardin, B. Developmental toxicity of nine selected compounds following prenatal exposure in the mouse: naphthalene, *p*-nitrophenol, sodium selenite, dimethylphthalate, ethylene thiourea, and four glycol ether derviatives. *J. Toxicol. Environ. Health* **1985**, *15*, 25−38.

Plopper, C.; Suverkropp, C.; Morin, D.; Buckpitt, A. Relationship of cytochrome P-450 activity to Clara cell cytotoxicity. I. Histopathologic comparison of the respiratory tract of mice, rats and hamsters after parenteral administration of naphthalene. *J. Pharmacol. Exp. Ther.* **1992**, 261, 353−363.

Quick, D. J. Modifications of a physiological model for naphthalene in mice and rats and adaptation to a novel cell culture system. M.S. Thesis, Cornell University, Ithaca, NY, 1996.

Ramsey, J.; Andersen, M. A physiologically based description of the inhalation pharmacokinetics of styrene in rats and humans. *Toxicol. Appl. Pharmacol.* **1984**, *73*, 159−175.

Richieri, P.; Buckpitt, A. Efflux of naphthalene oxide and reactive naphthalene metabolites from isolated hepatocytes. *J. Pharmacol. Exp. Ther.* **1987**, *242*, 485−492.

Rietjens, I.; Dormans, J.; Rombout, P.; Van Bree, L. Qualitative and quantitative changes in cytochrome P-450-dependent xenobiotic metabolism in pulmonary microsomes and isolated Clara cell populations derived from ozone exposed rats. *J. Toxicol. Environ. Health*. **1988**, *24*, 515−531.

Seglen, P. Preparation of rat liver cells, III. Enzymatic requirements for tissue dispersion. *Exp. Cell. Res.* **1973**, *82*, 391−398.

Seidegard, J.; DePierre, J.; Moron, M.; Johannesen, K.; Ernster, L. Characterization of rat lung epoxide (styrene oxide) hydrase with a modified radioactive assay of improved sensitivity. *Cancer Res.* **1977**, *37*, 1075−1082.

Shank, R.; Barrowa, L.; Buckpitt, A. Comparative metabolism of hydrazine and naphthalene. AFARMAL-TR-80-103, 1980.

Stillwell, W.; Horning, M.; Griffin, G.; Tsang, W.-S. Identification of new sulfur-containing metabolites of naphthalene in mouse urine. *Drug Metab. Dispos.* **1982**, *10*, 624−631.

Suga, T.; Ohata, I.; Akagi, M. Studies on mercapturic acids: Effect of some aromatic compounds on the level of glutathione and the activity of glutathionase in the rat. *J. Biochem*. **1966**, *59*, 209−215.

Summer, K.; Rozman, K.; Coulston, F.; Greim, H. Urinary excretion of mercapturic acids in chimpanzees and rats. *Toxicol. Appl. Pharmacol.* **1979**, *50*, 207−212.

Sweeney, L. M. Development of a multicompartmental, multiple cell type bioreactor and corresponding pharmacokinetic model for naphthalene. Ph.D. Thesis, Cornell University, Ithaca, NY, 1993.

Sweeney, L.; Shuler, M.; Quick, D.; Babish, J. A preliminary physiologically based pharmacokinetic model for naphthalene and naphthalene oxide in mice and rats. *Annals Biomed. Eng.* **1996**, *24*, 305−320.

Tingle, M.; Pirmohamed, M.; Templeton, E.; Wilson, A.; Madden, S.; Kitteringham, N.; Park, B. K. An investigation of the formation of cytotoxic, genotoxic, protein-reactive and stable metabolites from naphthalene by human liver microsomes. *Biochem. Pharm*. **1993**, *46*, 1529−1538.

Toxicological Profile for Naphthalene and 2-Methylnaphthalene. U.S. Agency for Toxic Substances and Disease, 1990.

Tsuruda, L.; Lame, M.; Buonarati, M.; Buckpitt, A. Detection of naphthalene oxide (NO) in whole blood after ip administration of the bronchiolar cytotoxicant naphthalene (NA). *FASEB J*. **1990**, *4*, A609.

Warren, D.; Brown, D., Jr.; Buckpitt, A. Evidence for cytochrome P-450 mediated metabolism in the bronchiolar damage by naphthalene. *Chem.-Biol. Interact.* **1982**, *40*, 287−303.

Weibel, E.; Staubli, W.; Gnagi, H.; Hess, F. Correlated morphometric and biochemical studies on the liver cell. *J. Cell Biol.* **1969**, *42*, 68ff.

Wilson, A. S.; Tingle, M. D.; Kelly, M. D.; Park, B. K. Evaluation of the generation of genetoxic and cytotoxic metabolites of benzo[*x*]pyrene, aflatoxin B., naphthalene and tamoxifen using human liver microsomes and human lymphocytes. *Hum. Exp. Toxicol.* **1995**, *14*, 507−515.

Wilson, A. S.; Davis, C. D.; Willimas, D. P.; Buckpitt, A. R.; Pirmohamed, M.; Park, B. K. Characterization of the toxic metabolites of naphthalene. *Toxicology* **1996**, *114*, 233−242.

Wish, L.; Furth, J.; Storey, R. Direct determination of plasma, cell, and organ- blood volumes in normal and hypervolemic mice. *Proc. Soc. Exp. Biol. Med.* **1950**, *74*, 644−648.

Zheng, J.; Cho, M.; Jones, A. D.; Hammock, B. D. Evidence of quinone metabolites of naphthalene covalently bound to sulfur nucleophiles of proteins of murine Clara cells after exposure to naphthalene. *Chem. Res. Toxicol.* **1997**, *10*, 1008−1014.

Accepted April 1, 1999.

BP990057T